ISSN 1070-4280, Russian Journal of Organic Chemistry, 2021, Vol. 57, No. 8, pp. 1352–1360. © Pleiades Publishing, Inc., 2021.

Synthesis, Characterization, Antimicrobial Activity Screening, and Molecular Docking Study of Pyrimidine Carbonitrile Derivatives

Radhika Bhat[a] and Noor Shahina Begum[a,*]

[a] *Department of Studies in Chemistry, Bangalore University, Bangalore, 560056 India*
**e-mail: noorsb05@gmail.com; noorsb@bub.ernet.in*

Received November 06, 2020; revised November 27, 2020; accepted November 28, 2020

Abstract—The present work describes the synthesis of 4-amino-6-(2-benzylidenehydrazinyl)-pyrimidine-5-carbonitrile derivatives, 4-amino-6-[(2-phenylethyl)amino]pyrimidine-5-carbonitrile, and 4-amino-6-(piperidin-1-yl)pyrimidine-5-carbonitrile. The compounds were characterized by FT-IR and ^{1}H and ^{13}C NMR spectroscopy and mass spectrometry. All the compounds were evaluated for in vitro antimicrobial activity against different bacterial and fungal strains. The minimum inhibitory concentrations (MICs) of all the compounds were validated. 4-Amino-6-[2-(3,4-dimethoxybenzylidene)hydrazinyl]pyrimidine-5-carbonitrile and 4-amino-6-(piperidin-1-yl)-pyrimidine-5-carbonitrile, which have the lowest MIC values were selected for cell leakage analysis and bacterial growth curve study. It was found that both the compounds have potential to induce bacterial cell membrane rupture and disintegration. Field emission scanning electron microscopic analysis confirmed the effect of the selected compounds on the morphology of both Gram-positive (*S. aureus*) and Gram-negative (*E. coli*) bacteria. The mechanism of interaction between the drug and the target protein of *S. aureus* and *E. coli* was studied by molecular docking.

Keywords: pyrimidine-5-carbonitrile, antimicrobial activity, cell leakage analysis, FE-SEM, molecular docking

DOI: 10.1134/S1070428021080169

INTRODUCTION

The scope for the development of new classes of antimicrobial agents is high, as many of the pathogenic microorganisms have acquired resistance against currently used drugs. Also, the emergence of new infectious diseases has significantly increased the demand for novel and potent molecules to combat microbial infections. Pyrimidines, a class of molecules comprising a heterocyclic ring and two nitrogen atoms in their structure, display a wide range of biological and pharmaceutical activities, including anti-inflammatory [1–3], analgesic [2], antioxidant [4], antiviral [5, 6], anti-amoebic [7], CDK2 inhibitory [8], antitubercular [9], anticancer [10–12], antidiabetic [13], antitumor [14], anti-hyperglycemia [15], and in vivo diuretic [16] activities.

A great number of pyrimidine derivatives have been studied for their antimicrobial activity over the past few years [17]. Different classes of mono-, di-, tri-, and tetra-substituted pyrimidines showed antimicrobial activities against various strains of bacteria and fungi [17]. A wide range of trisubstituted pyrimidines were earlier evaluated for their in vitro antimicrobial activity, and the activity of 2,4,6-trisubstituted pyrimidine derivatives against both bacteria and fungi compared with that of standard drugs [18]. Desai et al. [19] have synthesized and analyzed the in vitro antibacterial activity of a novel series of 2-amino-4-(4-chlorophenyl)-6-substituted-pyrimidines and observed potent antibacterial activity against both gram-negative (*E. coli*, *Salmonella*) and gram-positive (*Bacillus pumilus*, *micrococcus*) bacteria.

In search of novel and potent antimicrobial agents, in the present work we have synthesized novel pyrimidine carbonitrile derivatives and screened them for antimicrobial activity against various bacterial and fungal strains.

RESULTS AND DISCUSSION

The target 4-amino-6-(2-benzylidenehydrazinyl)-pyrimidine-5-carbonitrile derivatives **4a–4d**, 4-amino-

Scheme 1.

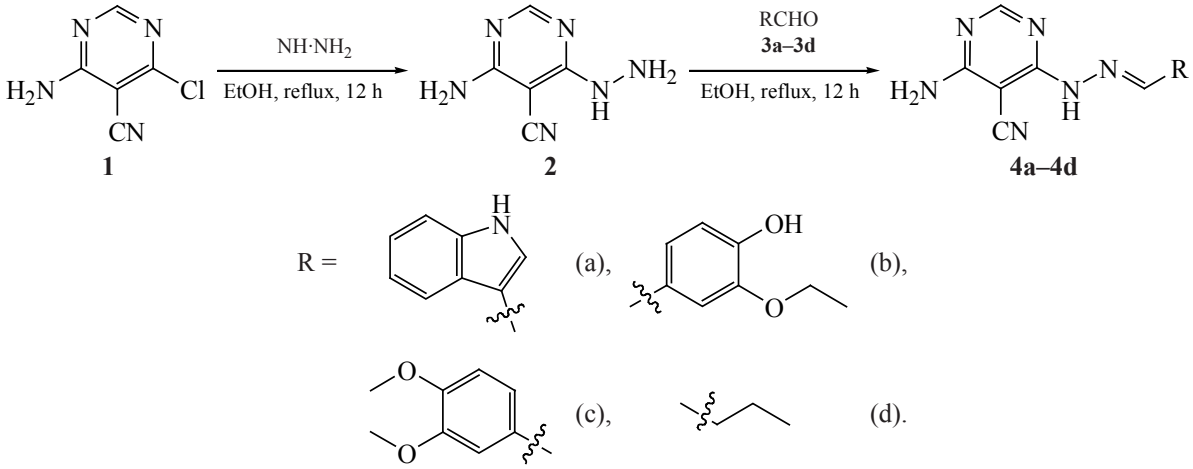

6-[(2-phenylethyl)amino]pyrimidine-5-carbonitrile (**5**), and 4-amino-6-(piperidin-1-yl)pyrimidine-5-carbonitrile (**6**) were synthesized as shown in Schemes 1–3, respectively. Scheme 1 represents the synthesis of compounds **4a–4d** by the reaction of 4-amino-6-chloropyrimidine-5-carbonitrile (**1**) with hydrazine hydrate in ethanol to obtain 4-amino-6-hydrazinylpyrimidine-5-carbonitrile (**2**) followed by the condensation with various substituted aldehydes. Compound **5** was obtained by the reaction of compound **1** with (2-phenylethyl)amine in DMF in the presence of Et_3N (Scheme 2). Compound **6** was synthesized by the reaction of compound **1** with piperidine in ethanol (Scheme 3).

The structures of compounds **2**, **4a–4d**, **5**, and **6** were confirmed by IR and NMR spectroscopy and mass spectrometry. The IR spectra of the all the synthesized compounds displayed bands at 3409 to 3076 cm^{-1}, assigned due to NH stretching vibrations and 2359 to 2201 cm^{-1}, assigned to C≡N stretching vibrations. The bands at 1666 to 1651 cm^{-1} in the spectra of compounds **4a–4d** are characteristic of the C=N group.

The ^1H NMR spectrum of compound **2** displayed signals at 7.63 and 7.96 ppm, assignable to the hydrazine moiety $–NHNH_2$ and the NH_2 group attached to the pyrimidine ring. The ^1H NMR spectra of compounds **4a–4d** contained a singlet NH signal at 11.14 to 11.69 ppm. The amino group of pyrimidine derivatives **4a–4d** gives two-hydrogen singlets in the range 7.00 to 11.27 ppm, and the singlet signal at 7.45 to 9.37 ppm was assigned to the imine CH proton. The ^1H NMR spectrum of compound **5** shows peaks at 7.38 ppm, assignable to two $–NH_2$ protons and at 5.39 ppm, assignable to the proton of the NH group bonded to the alkyl moiety. The ^1H NMR of compound **6** displays a singlet at 8.01 ppm from one pyrimidine CH proton, a broad singlet at 7.21 ppm from two NH_2 protons, a triplet

Scheme 2.

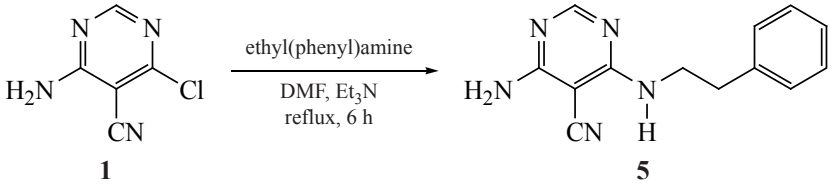

Scheme 3.

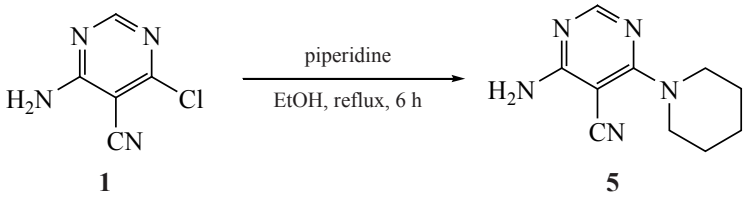

Table 1. Minimum inhibitory concentrations of substituted pyrimidine derivatives **4a–4d**, **5**, and **6** against bacterial strains

Comp. no.	MIC, μg/mL			
	B. subtilis	*E. coli*	*S. aureus*	*S. typhi*
4a	100	100	100	80
4b	80	100	100	80
4c	25	50	50	50
4d	200	200	200	250
5	180	200	120	120
6	50	25	25	50
Ampicillin	50	50	50	50

at 3.76 ppm from four protons of the piperidine ring, and a multiplet at 1.73–1.48 ppm from the remaining six piperidine protons.

In the ^{13}C NMR analysis for compounds **2**, **4a–4d**, **5**, and **6**, there were signals at 117 attributed to the C≡N group attached to the aromatic ring. There were signals between 157.9 to 168.3 ppm, which were assigned to the pyrimidine C=N carbons. The mass spectral data were consistent with the proposed structure of the synthesized compounds. The crystal structure of compound **6** was reported in [28].

The synthesized compounds **4a–4d**, **5**, and **6** were screened for their antimicrobial activity against four bacteria and two fungal strains as per CLSI guidelines. The test bacteria comprised two Gram-positive bacteria *S. aureus* (ATCC 29213) and *B. subtilis* (NCTC 8236) and two Gram-negative bacteria *E. coli* (ATCC 10536) and *S. typhi*. The two fungal strains comprised *A. flavus* (NCIM539) and *A. niger* (NCIM1196). Ampicillin and fluconazole were used as standard drugs for antibacterial and antifungal activity screening, respectively. The antibacterial and antifungal activity was measured in terms the minimum inhibitory concentration (MIC) (Tables 1 and 2).

Table 2. Minimum inhibitory concentrations of substituted pyrimidine derivatives **4a–4d**, **5**, and **6** against fungal strains

Comp. no.	MIC, μg/mL	
	A. niger	*A. flavus*
4a	100	100
4b	100	80
4c	50	50
4d	100	100
5	200	150
6	25	25
Fluconazole	25	25

All the synthesized compounds showed good to moderate levels of antibacterial and antifungal activity. Compounds **4c** and **6** were more potent than the other compounds against bacterial strains, and compound **6** proved to be the most potent against all microbial pathogens. The MIC values of **4c** and **6** fell in the range 25–50 μg/mL for both bacteria and fungi, which compares with the respective values for standard drugs. Compound **4b** exhibited a lower antibacterial activity compared to **4c** and **6**, while compounds **4a** and **4d** did not give a significant zone of inhibition against the test fungal strains. Compound **4d** was the least active against the test bacterial strains. Compounds **4a** and **5** showed moderate antimicrobial activity compared to standard used. The resulting data showed that compounds **4c** and **6** hold promise as potential antibacterial and antifungal agents, and just these compounds were chosen for further research.

The ability of compounds **4c** and **6** to induce bacterial cell lysis was evaluated by the cell leakage assay. Nucleotides leaked from bacterial cells were measured by plotting the optical density at 320 nm at different exposure times (up to 24 h with 4-h intervals). The results confirmed that both the test compounds induce a time-dependent increase in the rate of leakage of cell nucleotides in both *E. coli* and *S. aureus*. Results are depicted in Fig. 1.

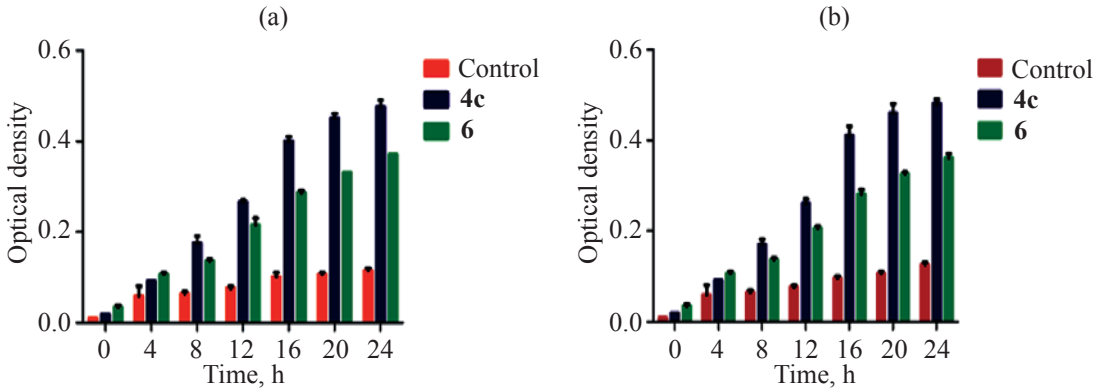

Fig. 1. Cell leakage study of compounds **4c** and **6** on (a) *E. coli* and (b) *S. aureus*.

The effect of compounds **4c** and **6** on the bacterial growth curve was evaluated on *E. coli* and *S. aureus* bacteria. The control bacterial culture showed a typical growth pattern with a lag phase of 4 h and a log phase of 8–10 h. Treatment with the IC_{50} concentrations of compounds **4c** and **6** induced significant changes in the normal bacterial growth pattern. The lag phase of bacteria significantly decreased to 5–6 h (Fig. 2). This result provided clear evidence for the antibacterial potential of both test compounds against the pathogens studied.

The effect of compound **4c** and **6** on the morphology of *S. aureus* and *E. coli* cells was evaluated by field emission scanning electron microscopy (FESEM) (Figs. 3 and 4). The FE-SEM images of control untreated cells showed smooth cell surfaces with normal morphological characteristics. Treatment with both test compounds led to a significant deterioration in the cell wall, which in turn led to disintegration of cell membrane. These findings gave further evidence showing that compounds **4c** and **6** cause lysis of *S. aureus* and *E. coli* cells.

Penicillin-binding proteins (PBPs) are the targets for the antibiotics, as they play a major role in the bacterial cell wall synthesis. Beta-lactam antibiotics bind to the active site of the PBPs and thus inhibit the cross-linking of peptidoglycans, leading to bacterial death [20]. In the present study, based on the MIC assay and docking analysis, we selected to study the mode of binding of the synthesized molecules with PBPs. The ligands were allowed to interact with a PBP of *B. subtilis*. The standard antibiotic drug ampicillin was used as control.

In silico docking analysis was performed between ligands **4c** and **6**, ampicillin, and the PBP4a of *B. subtilis*. The crystal structure of the PBP4a of *B. subtilis* was retrieved from the RCSB-PDB database

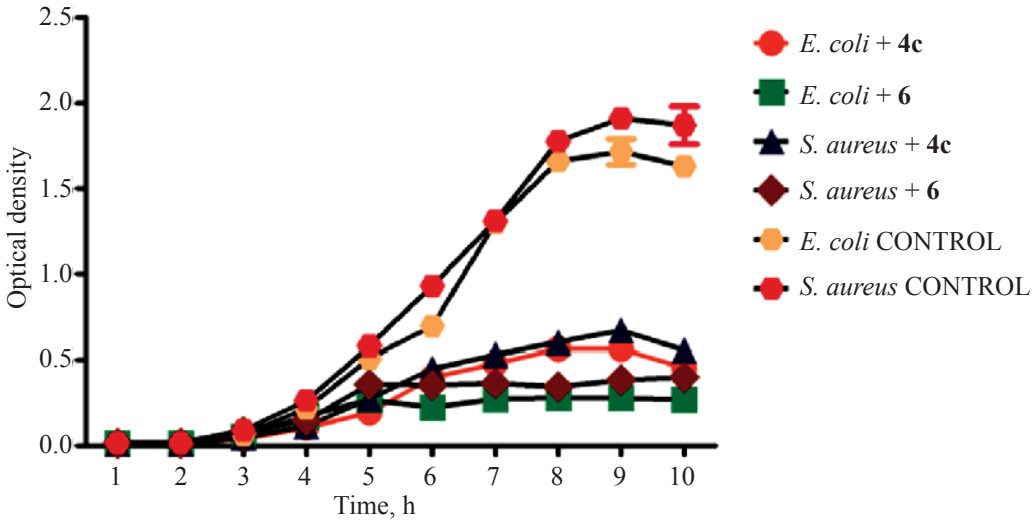

Fig. 2. Bacterial growth curve analysis of compounds **4c** and **6**.

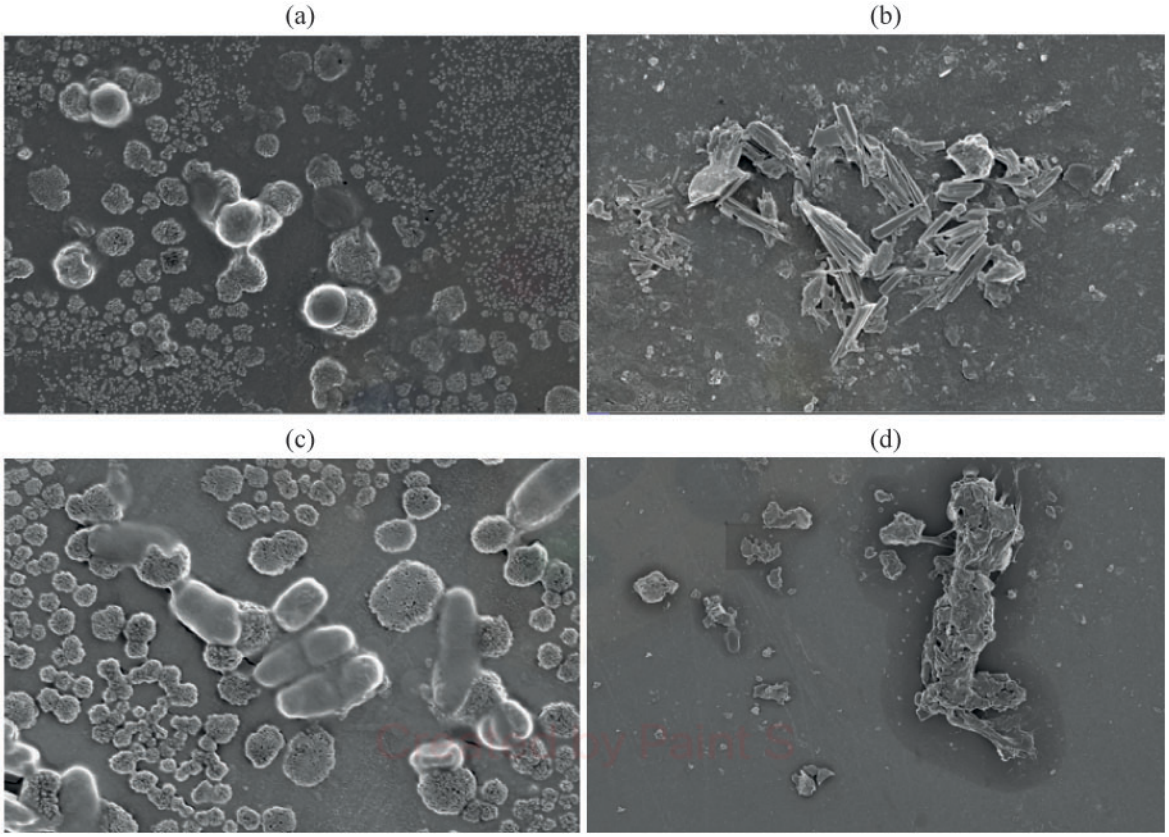

Fig. 3. FESEM images demonstrating the effect of compound **4c** on the morphology of *S. aureus* and *E. coli* bacterial cell walls: (a) control *S. Aureus*; (b) *S. Aureus* after incubation with compound **4c**; (c) control *E. coli*, and (d) *E. coli* after incubation with compound **4c**.

(PDB ID-1W5D) in the .pdb format. The structural refinement of the protein was performed using Galaxy Refine [21] and further subjected to Ramachandran plot analysis using PROCHECK software [22]. The refined protein was loaded to AutoDock vina [23] of the PyRx software for docking analysis. The structures of ligands **4c**, **6**, and ampicillin were drawn in Marvin sketch and saved in the .sdf format. Energy minimization was performed using the Open Babel [24] in PyRx0.8. The grid box was set to the XYZ coordinates of 45.67, 37.89, and 93.54, respectively, and the box dimensions were 73.67, 85.31, and 47.62 along the XYZ axis, respectively, to cover the entire protein. The protein–ligand interaction of the conformation complex with the lowest AutoDock vina score was visualized using PyMOL 1.3, and the interaction was analyzed using LIGPLOT^{+} software [25].

All PDBs contain serine in the active site. The PBP4a of *B. subtilis* (1W5D) has serine at position 52 [26]. The results of docking of compounds **4c**, **6**, and ampicillin to 1W5D, the interactions with Ser52 are highly conserved. Ligand **4c** forms two hydrogen bonds (3.14 and 3.17 Å) with Ser52 and one with Thr412 (3.17 Å) (Fig. 5, A/A1). The higher the number of hydrogen bonds, the more specific is binding of a ligand to a target protein [27]. Ligand **6** forms one hydrogen bond with Ser52 (3.13 Å) (Fig. 5, B/B1). However, the reference ligand ampicillin forms one hydrogen bond with Ser52 (3.32 Å) and another with Ser299 (3.32 Å) (Fig. 5, C/C1). Along with hydrogen bonding, the ligands enter hydrophobic interactions, where Tyr150, Asn301, and Ser414 are highly conserved in all the three interactions depicted in Fig. 5.

As judged from the MIC values and docking results (Tables 1 and 3), ligand **4c** has a higher binding affinity to PBPs compared to ligand **6** and the standard drug ampicillin.

In summary, we have synthesized 4-amino-6-(2-benzylidenehydrazinyl)-pyrimidine-5-carbonitrile derivatives **4a–4d**, 4-amino-6-[(2-phenylethyl)amino]-pyrimidine-5-carbonitrile (**5**), and 4-amino-6-(piperidin-

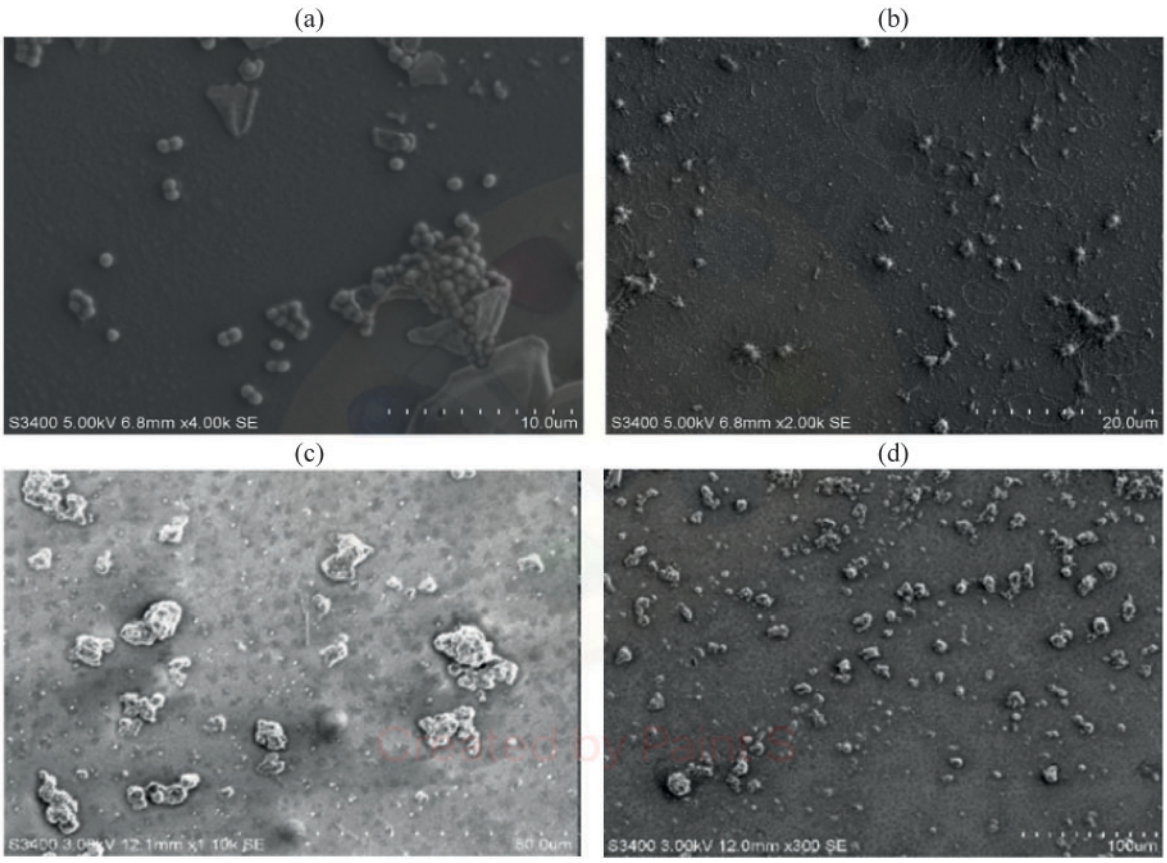

Fig. 4. FESEM images demonstrating the effect of compound **6** on the morphology of *S. aureus* and *E. coli* bacterial cell walls: (a) control *S. Aureus*; (b) *S. Aureus* after incubation with compound **6**; (c) control *E. coli*, and (d) *E. coli* after incubation with compound **6**.

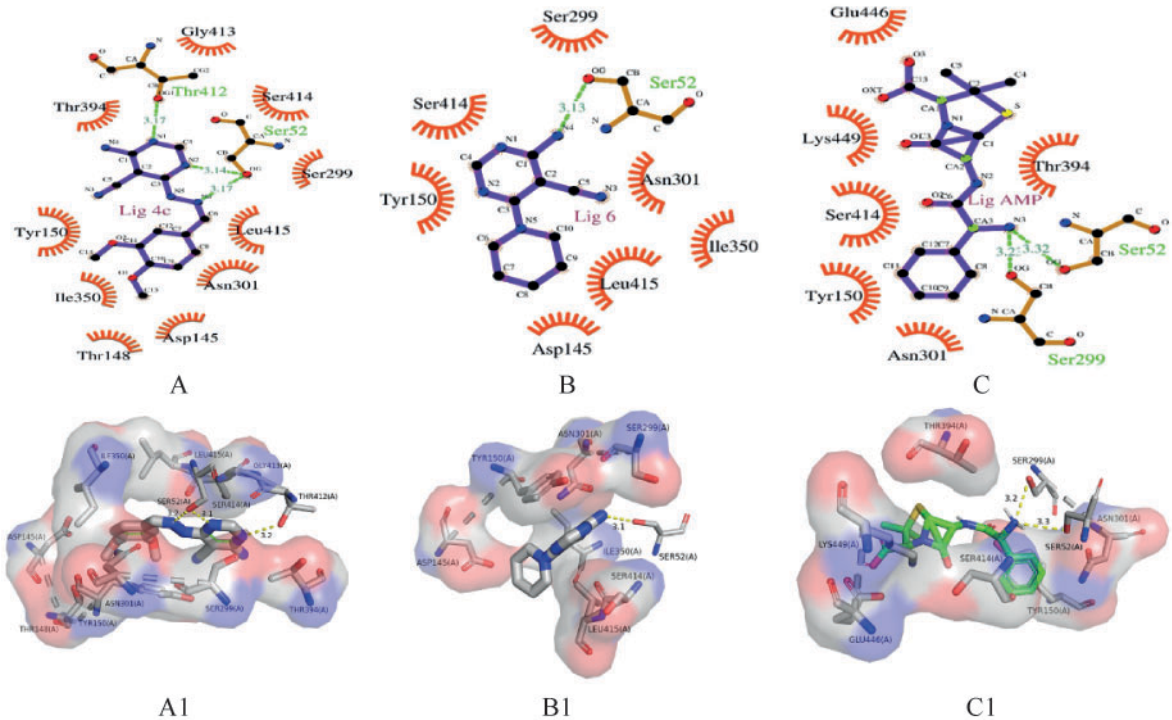

Fig. 5. In silico molecular docking of (A/A1) compound **4c**, (B/B1) compound **6**, and (C/C1) ampicillin to the PBP4a of *B. subtilis*. Hydrophobic interactions are represented as red semi-circles with spokes, and hydrogen bonds are represented as dotted lines.

Table 3. Docking interaction analysis of 1W5D with ligands **4c**, **6**, and ampicillin

Ligand	Vina score, kcal/mol	Binding site residues
4c	–6.9	Ser52 (3.14 and 3.17 Å), Asp145, Thr148, Tyr150, Ser299, Asn301, Ile350, Thr394, Thr412 (3.17 Å), Gly413, Ser414, Leu415
6	–5.5	Ser52 (3.13 Å), Asp145, Tyr150, Ser299, Asn301, Ile350, Ser414, Leu415
Ampicillin	–6.5	Ser52 (3.32 Å), Tyr150, Ser299 (3.23 Å), Asn301, Thr394, Ser414, Glu446, Lys449

1-yl)pyrimidine-5-carbonitrile (**6**). All the synthesized compounds were screened for their antimicrobial activity against *S. aureus* and *B. subtilis* (Gram-positive) and *E. coli* and *S. typhi* (Gram-negative) bacterial strains and *A. flavus* and *A. niger* fungal strains. All the compounds showed good to moderate levels of antibacterial and antifungal activity, and compounds **4c** and **6** proved the most potent antimicrobial agents with lowest MIC values. Compounds **4c** and **6** have a potential to induce bacterial cell membrane rupture and disintegration. The mode of action was explored by FESEM imaging, which clearly indicated the membrane damaging effects of compounds **4c** and **6**. In silico molecular docking gave evidence showing that compound **4c** has a higher binding affinity to PBPs compared to compound **6** and the standard drug ampicillin. Compounds **4c** and **6** hold promise as potent antimicrobial agents.

EXPERIMENTAL

Commercial reagents and solvents were used without any further purification. The melting points were measured in open capillaries using a Guna melting point apparatus and are uncorrected. The IR spectra were run on a Nicolet iz10 FTIR spectrophotometer. The ^{1}H and ^{13}C NMR spectra were recorded on a Bruker 400 spectrometer at 400 MHz in DMSO-d_6 (Sigma-Aldrich), internal standard TMS. The reaction progress was monitored on TLC silica gel plates. The mass spectra were obtained on an Agilent Technologies 6110 Quadrupole LC/MS instrument. Field emission scanning electron microscopy (FESEM) was performed on a GEMINI SEM 300 Nano VP scanning electron microscope.

4-Amino-6-hydrazinylpyrimidine-5-carbonitrile (2). A mixture of 2.0 g (0.01298 mmol) of 4-amino-6-chloropyrimidine-5-carbonitrile (**1**) and 3.3 g (0.10384 mmol) of hydrazine hydrate was refluxed in 40 mL of dry ethanol (0.2 mmol) for 12 h. On completion of the reaction (by TLC), the reaction mixture was cooled to room temperature. The precipitate that formed was filtered off, washed with ethanol, dried, and recrystallized from ethanol. Yield 84%, off-white solid, mp 270–273°C. IR spectrum, ν, cm^{-1}: 3409 (NH), 3083 (Ar–CH), 2208 (C≡N), 1666 (C=N), 1321 (C–N). ^{1}H NMR spectrum, δ, ppm: 3.73 d (1H, NH, *J* 16.0 Hz), 7.08 s (1H, Pm-H), 7.62 d (2H, NH_2, *J* 8.0 Hz), 7.96 d (2H, NH_2, *J* 16.0 Hz). ^{13}C NMR spectrum, δ, ppm: 117.0, 157.9, 166.4, 174.9. Mass spectrum (LCMS), *m/z*: 151.1 $[M]^+$. Found, %: C 40.90; H 4.17; N 55.92. $C_5H_6N_6$. Calculated, %: C 40.00; H 4.03; N 55.97.

4-Amino-6-(2-benzylidenehydrazinyl)pyrimidine-5-carbonitriles 4a–4d (*general procedure*). Substituted aldehyde **3a–3d** (0.0079 mmol) was added to a solution of 0.2 g (0.0066 mmol) of 4-amino-6-hydrazinylpyrimidine-5-carbonitrile (**2**) in 10 mL of ethanol, and the reaction mixture was refluxed for 12 h. On completion of the reaction (by TLC), the reaction mixture was cooled to room temperature. The precipitate that formed was filtered off, washed with ethanol, and dried to obtain target product **4a–4d**.

4-Amino-6-[2-(3*H*-indol-3-yl-methylene)hydrazinyl]pyrimidine-5-carbonitrile (4a). Yield 80%, light yellow solid, mp 247–248°C. IR spectrum, ν, cm^{-1}: 3361 (NH), 3142 (Ar–H), 2201 (C≡N), 1651 (C=N), 1335 (C–N). ^{1}H NMR spectrum, δ, ppm: 8.04 s (1H, imine-CH), 7.07–8.54 m (6H, Ar-H), 8.91 s (1H, Pm-H), 11.27 s (2H, NH_2), 11.60 s (1H, NH). ^{13}C NMR spectrum, δ, ppm: 68.3, 112.8, 117.8, 121.2, 123.9, 125.6, 126.9, 131.3, 132.5, 138.6, 142.7, 155.6, 160.8, 166.8. Mass spectrum (LCMS), *m/z*: 279.1 $[M]^+$. Found, %: C 60.16; H 4.72; N 35.18. $C_{14}H_{13}N_7$. Calculated, %: C 60.20; H 4.69; N 35.10.

4-Amino-6-[2-(3-ethoxy-4-hydroxybenzylidene)-hydrazinyl]pyrimidine-5-carbonitrile (4b). Yield 75%, white solid, mp 220–224°C. IR spectrum, ν, cm^{-1}: 3326, 3143 (NH), 3520 (OH), 2204 (C≡N), 1656 (C=N), 1237 (C–N), 1177 (C–O). ^{1}H NMR spectrum,

δ, ppm: 1.30 t (3H, CH_3, *J* 8.0 Hz), 4.07–4.19 m (2H, OCH_2), 6.80 s (1H, OH), 6.98 s (1H, Ar-H), 7.00 br.s (2H, NH_2), 7.61 s (1H, Ar-H), 7.95 s (1H, Ar-H), 8.05 s (1H, Pm-H), 9.37 s (1H, =CH), 11.57 s (1H, NH). ^{13}C NMR spectrum, δ, ppm: 64.3, 79.2, 100.2, 114.9, 116.5, 118.1, 123.2, 128.2, 143.8, 148.3, 151.3, 161.1, 162.4, 168.3. Mass spectrum (LCMS), *m/z*: 300.2 $[M]^+$. Found, %: C 55.73; H 5.86; N 27.85; O 10.68. $C_{14}H_{16}N_6O_2$. Calculated, %: C 55.99; H 5.37; N 27.98; O 10.66.

4-Amino-6-[2-(3,4-dimethoxybenzylidene)hydrazinyl]pyrimidine-5-carbonitrile (4c). Yield 78%, light yellow solid, mp 215–218°C. IR spectrum, ν, cm^{-1}: 3076 (NH), 2359 (C≡N), 1662 (C=N), 1239 (C–N), 1259 (C–O). ^1H NMR spectrum, δ, ppm: 3.97 d [6H, 2(OCH_3), *J* 8.0 Hz], 6.98 d (1H, Ar-H, *J* 8.0 Hz), 7.49 d (1H, Ar-H, *J* 8.0 Hz), 7.67 s (1H, Ar-H), 8.02 s (1H, =CH), 8.07 s (1H, Pm-H), 8.19 br.s (2H, NH_2), 11.69 br.s (1H, NH). ^{13}C NMR spectrum, δ, ppm: 56.6, 68.8, 109.0, 112.1, 113.1, 122.3, 125.1, 128.6, 143.8, 149.8, 151.2, 161.1, 162.0, 167.8. Mass spectrum (LCMS), *m/z*: 300.22 $[M]^+$. Found, %: C 55.63; H 5.52; N 27.93; O 10.62. $C_{14}H_{16}N_6O_2$. Calculated, %: C 55.99; H 5.37; N 27.98; O 10.66.

4-Amino-6-(2-butylidenehydrazinyl)pyrimidine-5-carbonitrile (4d). Yield 78%, white solid, mp 240–242°C. IR spectrum, ν, cm^{-1}: 3331, 3174 (NH), 2207 (C≡N), 1654 (C=N), 1267 (C–N), 2870, 2932 (CH). ^1H NMR spectrum, δ, ppm: 0.92 t (3H, CH_3, *J* 8.0 Hz), 1.55–2.24 m (4H, CH_2), 7.15 s (2H, NH_2), 7.45 s (1H, imine-CH), 8.01 s (1H, Pm-H), 11.14 s (1H, NH). ^{13}C NMR spectrum, δ, ppm: 13.9, 19.8, 34.1, 68.2, 117.2, 158.3, 161.4, 162.6, 167.5. Mass spectrum (LCMS), *m/z*: 206.1 $[M]^+$. Found, %: C 49.93; H 6.25; N 43.78. $C_8H_{12}N_6$. Calculated, %: C 49.99; H 6.29; N 43.72.

4-Amino-6-[(2-phenylethyl)amino]pyrimidine-5-carbonitrile (5). A mixture of 1.0 g (0.00649 mmol) of 4-amino-6-chloropyrimidine-5-carbonitrile (**1**), 10 mL (10 V) of DMF, 0.94 g (0.00779 mmol) of ethyl(phenyl) amine, and 1.0 g (0.00974 mmol) of triethylamine were refluxed for 6 h. Upon cooling, the mixture was poured into 20 mL of ice-cold water. The precipitate that formed was filtered off, washed with water, dried, and recrystallized from ethanol to obtain the target product. Yield 74%, white solid, mp 134–135°C. IR spectrum, ν, cm^{-1}: 3396, 3322 (NH), 2201 (C≡N), 1663 (C=N), 1289 (C–N), 1450 (CH). ^1H NMR spectrum, δ, ppm: 1.49 d (4H, $2CH_2$, *J* 8.0 Hz), 5.39 t (1H, NH, *J* 8.0 Hz), 7.19–7.31 m (5H, Ar-H), 7.37 d (2H, NH_2, *J* 4.0 Hz), 7.97 s (Pm-H). ^{13}C NMR spectrum, δ, ppm: 24.3, 52.1, 68.5, 116.3, 126.3, 126.4, 128.2, 145.5, 161.2, 163.2, 165.4. Mass spectrum (LCMS), *m/z*: 240.1 $[M]^+$. Found, %: C 61.63; H 5.59; N 33.13. $C_{13}H_{14}N_6$. Calculated, %: C 61.40; H 5.55; N 33.05.

4-Amino-6-(piperidin-1-yl)pyrimidine-5-carbonitrile (6). A mixture of 1.0 g (0.0065 mol) of 4-amino-6-chloropyrimidine-5-carbonitrile (**1**) and 2.75 g (0.0325 mol) of piperidine was refluxed in 20 mL dry ethanol for 6 h. The reaction mixture was then cooled and stirred for 2 h at room temperature. The precipitate that formed was filtered off, washed with ethanol, dried, and recrystallized from acetone to obtain the target product. Yield 74%, colorless crystals, mp 140–143°C. IR spectrum, ν, cm^{-1}: 3426, 3308 (NH), 2190 (C=N), 1646 (C=N), 1223 (CN). ^1H NMR spectrum, δ, ppm: 1.48–1.73 m (6H, $3CH_2$), 3.76 t (4H, $2CH_2$, *J* 8.0 Hz), 7.21 br.s (2H, NH_2), 8.01 s (1H, Pm-H). ^{13}C NMR spectrum, δ, ppm: 24.9, 26.8, 58.9, 118.1, 159.9, 164.3, 168.5. Mass spectrum (LCMS), *m/z*: 205.1 $[M]^+$. Found, %: C 59.28; H 6.49; N 34.43. $C_{10}H_{13}N_5$. Calculated, %: C 59.10; H 6.45; N 34.46.

ACKNOWLEDGMENTS

The authors are grateful to the Zeiss Microscopy Customer Center, Carl Zeiss India (Bangalore), for providing the FESEM facility.

CONFLICT OF INTEREST

The authors declare no conflict of interest

SUPPLEMENTARY INFORMATION

The online version contains supplementary material available at https://doi.org/10.1134/S1070428021080169.

REFERENCES

1. Dasari, S.R., Tondepu, S., Vadali, L.R., and Seelam, N., *Synth. Commun*., 2020, vol. 50, p. 2950. https://doi.org/10.1080/00397911.2020.1787449
2. Tolba, M.S., Ahmed, M., El-Dean, A.M.K., Hassanien, R., and Farouk, M., *J. Heterocycl. Chem*., 2017, vol. 66. https://doi.org/10.1002/jhet.3056
3. Abu-Hashem, A.A. and Youssef, M.M., *Molecules*, 2011, vol. 16, p. 1956. https://doi.org/10.3390/molecules16031956
4. Salem, M.S. and Errayes, A.O., *J. Chem. Res*., 2016, vol. 40, p. 299.

https://doi.org/10.3184/174751916X14605482579576

5. Ramiz, M.M.M., El-Sayed, W.A., Hagag, E., and Abdel-Rahman, A.A.H., *J. Heterocycl. Chem*., 2011, vol. 48, p. 1028. https://doi.org/10.1002/jhet.686
6. Bai, S., Liu, S., Zhu, Y., and Wu, Q., *Tetrahedron Lett*., 2018, vol. 59, p. 3179. https://doi.org/10.1016/j.tetlet.2018.07.020
7. Parveen, H., Hayat, F., Mukhtar, S., Salahuddin, A., Khan, A., Islam, F., and Azam, A., *Eur. J. Med. Chem*., 2011, vol. 46, p. 4669. https://doi.org/10.1016/j.ejmech.2011.05.055
8. Ibrahim, D.A. and El-Metwally, A.M., *Eur. J. Med. Chem*., 2010, vol. 45, p. 1158. https://doi.org/10.1016/j.ejmech.2009.12.026
9. Desai, N.C., Trivedi, A.R., Vaghani, H.V., Somani, H.C., and Bhatt, K.A., *Med. Chem. Res*., 2016, vol. 25, p. 329. https://doi.org/10.1007/s00044-015-1485-7
10. Kassab, A.E. and Gedawy, E.M., *Eur. J. Med. Chem*. 2013, vol. 63, p. 224. https://doi.org/10.1016/j.ejmech.2013.02.011
11. Al-Issa, S.A., *Saudi. Pharm. J*., 2013, vol. 21, p. 305. https://doi.org/10.1016/j.jsps.2012.09.002
12. Ghorab, M.M. and Alsaid, M.S., *Biomed. Sci*., 2016, vol. 27, p. 110.
13. Barakat, A., Soliman, S.M., Al-Majid, A.M., Lotfy, G., Ghabbour, H.A., Fun, H.-K., Yousuf, S., Choudhary, M.I., and Wadood, A., *J. Mol. Struct*., 2015, vol. 1098, p. 365. https://doi.org/10.1016/j.molstru.2015.06.037
14. Hassan, A.S., Mady, M.F., Awad, H.M., and Hafez, T.S., *Chin. Chem. Lett*., 2017, vol. 28, p. 388. https://doi.org/10.1016/j.cclet.2016.10.022
15. Fatahala, S.S., Mahgub, S., Taha, H., and Hameed, R.H.A-E., *J. Enzyme Inhib. Med. Chem*., 2018, vol. 33, p. 809. https://doi.org/10.1080/14756366.2018.1461854
16. Majeed, J. and Shaharyar, M., *J. Enzyme Inhib. Med. Chem*., 2011, vol. 26, p. 819. https://doi.org/10.3109/14756366.2011.557022
17. Sharma, V., Chitranshi, N., and Agarwal, A.K., *Int. J. Med. Chem*., 2014, vol. 2014, Article ID 202784. https://doi.org/10.1155/2014/202784
18. Ashok, D., Kumar, R.S., Mohan Gandhi, D., and Jayashree, A., *Russ. J. Gen. Chem*., 2016, vol. 86, p. 1396. https://doi.org/10.1134/S1070363216060268
19. Desai, V., Desai, C.M., and Patel, D., *J. Institut. Chemists*, 2005, vol. 11, p. 104.
20. Oztürk, H., OzkirimLi, E., and Özgür, A., *PLoS One*, 2015. https://doi.org/10.1371/journal.pone.0117874
21. Heo, L., Park, H., and Seok, C., *Nucleic Acids Res*., 2013, vol. 41, p. W384. https://doi.org/10.1093/nar/gkt458
22. Laskowski, R.A., Macarthur, M.W., Moss, D.S., and Thornton, J.M., *J. Appl. Crystallogr*., 1993, vol. 26, p. 283. https://doi.org/10.1107/S0021889892009944
23. Trott, O. and Olson, A.J. *J., Comput. Chem*., 2010, vol. 31, p. 1.
24. O'Boyle, N.M., Banck, M., James, C.A., Morley, C., Vandermeersch, T., and Hutchison, G.R., *J. Chem. Inform*., 2011, vol. 3, p. 1. https://doi.org/10.1186/1758-2946-3-33
25. Laskowski, R.A. and Swindells, M.B., *J. Chem. Inf. Model*., 2011, vol. 51, p. 2778. https://doi.org/10.1021/ci200227u
26. Sauvage, E., Duez, C., Herman, R., Kerff, F., Petrella, S., Anderson, J.W., Adediran, S.A., Pratt, R.F., Frиre, J.M., and Charlier, P., *J. Mol. Biol*., 2007, vol. 371, p. 528. https://doi.org/10.1016/j.jmb.2007.05.071
27. Klebe, G., *Drug Design*, 2013, p. 61. https://doi.org/10.1007/978-3-642-17907-5-4
28. Radhika, B., Shraddha, K.N., and Begum, N.S., *IUCrData*, 2020, vol. 5, x200385. https://doi.org/10.1107/S2414314620003855